J|A|C|S ARTICLES

Published on Web 02/02/2010

Coverage Effects on the Palladium-Catalyzed Synthesis of Vinyl Acetate: Comparison between Theory and Experiment

Florencia Calaza,[†] Dario Stacchiola,[‡] Matthew Neurock,*[,§] and Wilfred T. Tysoe*[,†]

Department of Chemistry and Biochemistry, and Laboratory for Surface Studies, University of Wisconsin-Milwaukee, Milwaukee, Wisconsin 53211, Department of Chemistry, Michigan Technological University, Houghton, Michigan 49931, and Departments of Chemical Engineering and Chemistry, University of Virginia, Charlottesville, Virginia 22904-4741

Received August 20, 2009; E-mail: Neurock@virginia.edu

Abstract: The high adsorbate coverages that form on the surfaces of many heterogeneous catalysts under steady-state conditions can significantly lower the activation energies for reactions that involve the coupling of two adsorbed intermediates while increasing those which result in adsorbate bond-breaking reactions. The influence of the surface coverage on the kinetics of metal-catalyzed reactions is often ignored in theoretical and even in some ultrahigh vacuum experimental studies. Herein, first principle density functional theoretical calculations are combined with experimental surface titration studies carried out over well-defined Pd(111) surfaces to explicitly examine the influence of coverage on the acetoxylation of ethylene to form vinyl acetate over Pd. The activation energies calculated for elementary steps in the Samanos and Moiseev pathways for vinyl acetate synthesis carried out on acetate-saturated palladium surfaces reveal that the reaction proceeds via the Samanos mechanism which is consistent with experimental results carried out on acetate-saturated Pd(111) surfaces. The rate-limiting step involves a β-hydride elimination from the adsorbed acetoxyethyl intermediate, which proceeds with an apparent calculated activation barrier of 53 kJ/mol which is in very good agreement with the experimental barrier of 55 $\pm$ 4 kJ/mol determined from kinetic measurements.

Introduction

The past decade has witnessed an exponential increase in the use of *ab initio* density functional theory (DFT) calculations to elucidate the adsorption geometry and reactivity of molecules on metal surfaces in order to understand catalytic as well as other surface processes such as gas sensing, electrochemistry, and tribology.[1] Density functional theory has been rigorously tested and compared to both experiment and higher-level theory for gas-phase molecular reactions thus providing an outstanding benchmark as to its accuracy. The ability to test the predictions of DFT for surface-catalyzed processes relies solely on comparisons with experimental data since the application of higher-level wave function methods is prohibitive. Most of the detailed comparisons between theory and experiment for surface-catalyzed systems have focused on small molecules for reactions carried out at low coverages. Many catalytic reactions, however, involve relatively large molecules, and almost always proceed at higher coverages on the metal surfaces of supported heterogeneous catalysts. There are few, if any, stringent comparisons between experimentally measured and theoretical activation energies for complex catalytic reactions at high coverages to test how well DFT reproduces experimental, elementary-step activation energies for heterogeneous catalytic reactions. Such a direct comparison is made in the following for the elementary steps in the palladium-catalyzed synthesis of the vinyl acetate monomer (VAM), which involves the reaction between surface acetate species, and oxygen species to form VAM and water directly.[2] Recent studies by Goodman et al.[3−5] demonstrate that this reaction is catalyzed by unique noncontiguous Pd sites isolated within a Au(100) surface. Recent theoretical calculations help to support this idea.[6,7] Our interest herein is focused on the pure Pd(111) substrate which is highly covered under working conditions.

Extensive ultrahigh vacuum work has been carried out to examine the chemistry of the reactants, ethylene[8] and acetic acid,[9] as well as the product, vinyl acetate,[10] alone on palladium surfaces. We have previously reported experimental evidence that this reaction appears to be initiated on palladium by the

[†] University of Wisconsin-Milwaukee.
[‡] Michigan Technological University.
[§] University of Virginia.

(1) van Santen, R. A.; Neurock, M. *Molecular Heterogeneous Catalysis: A Conceptual and Computational Approach*; John Wiley and Sons: New York, 2006.
(2) Stacchiola, D.; Calaza, F.; Burkholder, L.; Tysoe, W. T. *J. Am. Chem. Soc.* **2004**, *126*, 15384. Stacchiola, D.; Calaza, F.; Burkholder, L.; Schwabacher, A. W.; Neurock, M.; Tysoe, W. T. *Angew. Chem.* **2005**, *44*, 4572.
(3) Chen, M. S.; Kumar, D.; Yi, C. W.; Goodman, D. W. *Science* **2005**, *310*, 291.
(4) Han, P. S.; Axnanda, S.; Lyubinetsky, I.; Goodman, D. W. *J. Am. Chem. Soc.* **2007**, *129*, 14355.
(5) Kumar, D.; Chen, M. S.; Goodman, D. W. *Catal. Today* **2007**, *123*, 77.
(6) Garcia-Mota, M.; Lopez, N. *J. Am. Chem. Soc.* **2008**, *130*, 14406.
(7) Mazzone, G.; Rivalta, I.; Russo, N.; Sicilia, E. *Chem. Commun.* **2009**, *14*, 1852.
(8) Tysoe, W. T.; Nyberg, G. L.; Lambert, R. M. *J. Phys. Chem.* **1984**, *88*, 1960. Wang, L. P.; Tysoe, W. T.; Hoffmann, H.; Zaera, F.; Ormerod, R. M.; Lambert, R. M. *Surf. Sci.* **1990**, *94*, 4236. Stacchiola, D.; Burkholder, J.; Tysoe, W. T. *Surf. Sci.* **2002**, *511*, 215.

 10.1021/ja907061m

insertion of ethylene into the oxygen−metal bond of an adsorbed acetate species to form an acetoxyethyl−palladium intermediate.[2] This is followed by β-hydride elimination to yield vinyl acetate. This route was first proposed by Samanos.[11] In an alternative pathway, which was suggested by Moiseev,[12] the reaction is thought to be initiated by the activation of ethylene to form a surface vinyl intermediate, which can subsequently insert directly into the adsorbed acetate to form vinyl acetate. Herein we carry out rigorous titration experiments and first principle density functional theoretical calculations to examine the elementary steps involved in both mechanisms and the influence of coverage in order to establish the controlling mechanism.

Experimental Methods

Infrared data were collected using a system that has been described previously[13] The sample could be resistively heated to 1200 K or cooled to 80 K by thermal contact with a liquid nitrogen-filled reservoir. Infrared spectra were collected using a Bruker Equinox infrared spectrometer and a liquid nitrogen-cooled, mercury cadmium telluride detector. The complete light path was enclosed and purged with dry, CO_2-free air. The C_2H_4 (Matheson, Research grade) and acetic acid (Aldrich, 99.99+ %), were transferred to glass bottles, which were attached to the gas-handling line for introduction into the vacuum chamber. Kinetic measurements were carried out by initially saturating the Pd(111) surface with acetate species by exposure to acetic acid. A flux of ethylene impinged onto the sample from a collimated dosing source to obtain an enhanced flux at the Pd(111) single crystal surface while minimizing the background pressure using an ethylene pressure of 2×10^{-4} Torr.[2] This ethylene pressure was selected to be sufficiently high that no variation in acetate reaction rate was observed as a function of ethylene pressure. The acetate removal kinetics were measured by monitoring the acetate asymmetric OCO vibrational mode at 1414 cm^{-12} by sequentially collecting spectra for 100 scans. The intense acetate OCO mode could easily be distinguished from other modes due to vinyl acetate (1788 cm^{-12}), ethylidyne (1330, 1090 cm^{-12}), and the acetoxyethyl intermediate (1718 cm^{-12}).

The high sticking probability of reactants at reaction conditions means that the total surface coverage of all surface species remains high throughout each titration experiment, thus ensuring very similar coverage effects. As the reaction proceeds, the surface acetate intermediates which are titrated away become replaced by ethylidyne.[2]

Theoretical Methods

First-principle density functional theoretical calculations were carried out using the periodic DMol3 code by Delley.[14,15] The wave function was expanded in terms of numerical basis sets of double numerical quality (DNP) with d-type polarization functions on each atom. The core electrons for the palladium atoms here were modeled using effective core pseudopotentials by Dolg[16] and Bergner[17] which explicitly treat scalar relativistic corrections. The wave functions were confined within a 3.5 Å real-space cutoff. The density was calculated using a multipolar expansion and integrated using a grid that contains up to 1000 points per atom. All calculations were performed spin unrestricted. The Perdew−Wang 91[18] form of Generalized Gradient Approximation (GGA) was used to model the gradient corrections to the correlation and exchange energies. The electronic energies were calculated using a $3 \times 3 \times 1$ k-point grid mesh to sample the first-Brillouin zone. The electronic density was converged within each self-consistent field iteration to within 1×10^{-4} au. To facilitate SCF convergence, Fermi statistics were used to determine the fractional electron occupation around the Fermi level. The energy in each geometry optimization cycle was converged to within 1×10^{-4} au. The gradient was converged to within 1×10^{-3} Å.

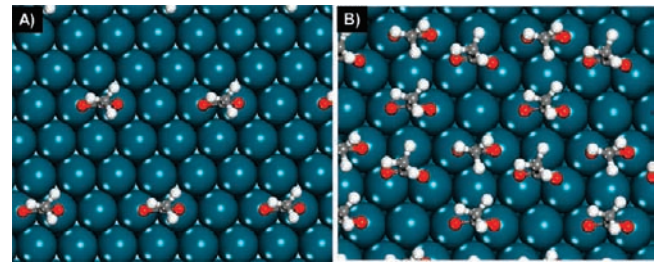

Figure 1. The optimized structures for the model high- (saturation) and low-coverage acetate/Pd(111) surfaces. A) 1/9 ML of acetate (low coverage), and B) 1/3 ML of acetate (saturation coverage).

The bulk lattice constant was optimized yielding a value of 2.753 Å, close to the experimental bulk lattice constant and was thus used in all subsequent calculations. The metal surface was modeled using a *3* × *3* unit cell comprised of 9 metal atoms per layer and four layers of Pd atoms with 18 Å of vacuum, which separates the slab in the z-direction. We examine both low coverages, defined here as 1/9 ML of acetate species, and the high saturation-coverage limit of acetate of 1/3 ML found experimentally by using 1 and 3 acetate molecules per unit cell, respectively. The structure of both the low and high coverages are shown in Figure 1 A and B, respectively. The 1/3 ML acetate coverage results in 66% of all of the Pd sites being occupied as each acetate is preferentially bound to two Pd atoms in a di-σ mode. The remaining two Pd atoms allow for the adsorption of ethylene. Higher coverages of acetate were found to be unstable. The adsorption of ethylene at the higher 1/3 ML acetate coverages induced a change in the structure of the adlayer to accommodate the ethylene. The acetate groups were found to preferentially adsorb in the structure depicted in Figure 2A in order to relieve the repulsive interactions that result due to the alignment of the acetate molecules.

The top two palladium layers were allowed to relax within the geometry optimization, whereas the lower two layers were held fixed at their bulk lattice positions. Adsorption energies were calculated by the following expression:

$$\Delta E_{Ads} = E_{VAM/Pd(111)} - E_{VAM} - E_{Pd(111)} \qquad (1)$$

where a negative value implies that the adsorption is exothermic.

(9) Zheng, T.; Stacchiola, D.; Poon, H. C.; Saldin, D. K.; Tysoe, W. T. *Surf. Sci.* **2004**, *564*, 71. Davis, J. L.; Barteau, M. A. *Langmuir* **1989**, *5*, 1299–1309. Davis, J. L.; Barteau, M. A. *Surf. Sci.* **1991**, *256*, 50.
(10) Calaza, F.; Stacchiola, D.; Neurock, M.; Tysoe, W. T. *Surf. Sci.* **2005**, *598*, 263. Li, Z.; Calaza, F.; Plaisance, C.; Neurock, M.; Tysoe, W. T. *J. Phys. Chem. C* **2009**, *113*, 9271.
(11) Samanos, B.; Boutry, P.; Montarnal, R. *J. Catal.* **1971**, *23*, 19.
(12) Moiseev, I. I.; Vargaftic, M. N.; Syrkin, Y. L. *Dokl. Akad. Nauk. USSR* **1960**, *133*, 377.
(13) Kaltchev; Thompson, A. W.; Tysoe, W. T. *Surf. Sci.* **1997**, *391*, 45.
(14) Delley, B. *J. Chem. Phys.* **1990**, *92*, 508. Delley, B. *J. Chem. Phys.* **2000**, *113*, 7756.
(15) *MaterialStudio*, V. 3.0; Accelyrys, Inc.: San Diego, CA, 2004.
(16) Dolg, M.; Wedis, U.; Stoll, H.; Preuss, H. *J. Chem. Phys.* **1987**, *86*, 866.
(17) Bergner, A.; Dolg, M.; Kuechle, W.; Stoll, H.; Preuss, H. *Mol. Phys.* **1993**, *80*, 143.
(18) Perdew, J. P.; Chevary, J. A.; Vosko, S. H.; Jackson, K. A.; Pederson, M. R.; Singh, D. J.; Fiolhais, C. *Phys. Rev. B* **1992**, *46*, 6671.

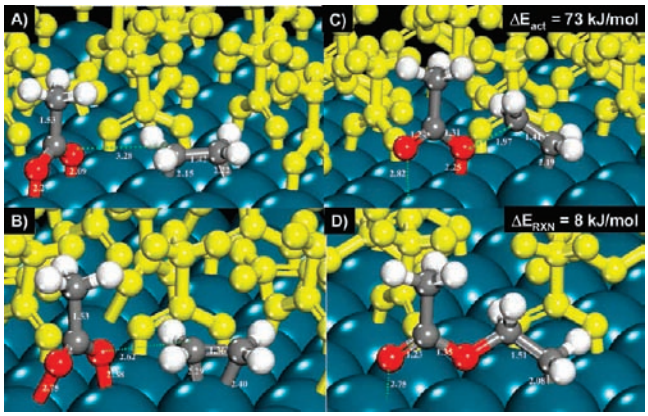

Figure 2. The optimized structures and energies for the coupling of ethylene and acetate at the high (saturation) coverages ($\Theta = 1/3$ ML of acetate). A) di-σ bound ethylene reactant, B) π-bound ethylene intermediate, C) transition state, and C) product state.

The transition states reported herein were determined using the LST/QST method established by Govind et al.[19] A linear transit is constructed based on 10 images between the optimized reactant and product states and used to maximize the energy along the reaction path. This is followed by a conjugate gradient minimization along all directions conjugate to the reaction path. This cycle is then carried out repeatedly with quadratic synchronous transit (QST) maximizations followed by conjugate gradient minimizations to isolate the transition state. Transition states were converged to within 0.1 eV/Å.

In order to elucidate the changes to the frontier molecular orbitals involved in the surface reaction chemistry, we extracted the central core cluster of the transition state comprising the four central Pd atoms, C_2H_4, and CH_3CO_2 fragments and used it to carry out single-point calculations. The calculations show how the occupancy of the orbitals changes within the transition state as the surface acetate coverage is increased. The scheme of Hirsfeld[18] was used to calculate the charges on each of the atoms in these clusters.

Results and Discussion

We previously reported on the adsorption and dissociation paths for ethylene,[21,22] acetic acid and acetate,[23,24] vinyl acetate,[2,10] and other key intermediates and their comparison with experiment.[2,10] We therefore do not discuss them in detail here. We focus here solely on the key C−O bond-forming and C−H bond-breaking reactions that control the Samonos and Moiseev mechanisms and provide a critical analysis of the effects of coverage on the key elementary steps in both reaction pathways. The activation energies were calculated for the Samanos pathway at both high and low acetate coverages.

Acetic acid readily dissociates onto Pd(111) to form 1/3 ML of acetate at saturation coverage. The activation barrier for this step was calculated to be less than 30 kJ/mol and less than 5 kJ/mol when assisted by surface oxygen or hydroxyl intermediates. The adsorption of ethylene on a clean Pd(111) surface was determined previously to be −62 kJ/mol,[25] which is in good agreement with the experimental results.[24] The adsorption energy on the saturated surface is significantly weaker with an energy of −20 kJ/mol. The activation barrier for the subsequent reaction between acetate and coadsorbed ethylene to form the acetoxyethyl intermediate was calculated to be 103 kJ/mol at a low coverage ($\Theta = 1/9$ ML), while at the higher acetate saturation coverage ($\Theta = 1/3$ ML) it decreases to 73 kJ/mol. The optimized reactant, transition and product structures along with the most critical bond lengths for each state are depicted in Figure 2. The transition state for this reaction, depicted in Figure 2B (for the high acetate coverage), involves the formation of a surface oxymetallocycle in which C−Pd and O−Pd atoms of the adsorbed ethylene and acetate are broken in order to form the C−O bond of the adsorbed acetoxyethyl intermediate. The reaction proceeds via the transformation of ethylene from a di-σ to a π-bound intermediate and then onto the acetate to form the acetoxyethyl intermediate.

At first glance, the decrease in activation energy at higher surface coverages is counterintuitive as both acetate and ethylene are nucleophiles; thus, higher acetate coverages would be expected to increase the activation barriers. At higher coverages, however, the adsorbed acetate intermediates compete with one another for electrons from the surface. As such, there is a decrease in the charge transfer from the metal to the oxygen atoms on the acetate. This leads to a more positive charge on the oxygen atoms of the acetate which thus reduces their nucleophilicity. The results from a Hirshfeld charge analysis on the transition states for both low and high coverages of acetate on the model Pd_4 cluster extracted from the optimized periodic structure shown in Figure 3 indicate that the charge on the O atom of acetate that reacts with the ethylene changes from −0.19 at low acetate coverages (1/9 ML) to −0.17 at the higher (1/3 ML) acetate coverages. While the positive charges on the Pd atoms increase at higher acetate coverage, it is not enough to meet the demand of the oxygen atoms on the acetate.

The activation barrier decreases for the coupling reaction since there is a loss of electron density from the antibonding σ^* state between the $2p_z$ orbitals on the carbon of ethylene and the $2p_z$ orbital on the oxygen of the acetate, which is occupied prior to the transition state. The frontier orbitals were therefore calculated for both the low- and high-acetate coverage transition states; the result are respectively depicted in A and B of Figure 4. At low coverages, the σ^* ($2p_C - 2p_O$) states are all fully occupied as is seen in the highest occupied molecular orbital present at −0.141 au in Figure 4A. The other states are much lower in energy and are therefore not shown as frontier orbitals. At higher coverages, however, nearly all of these states are pushed above the Fermi level in the transition states as shown in the lowest-unoccupied state at 0.1405 au in Figure 4B. Decreasing the number of electrons in the antibonding σ^* states significantly lowers the activation barrier. As a result, the barriers for bond-making steps decrease at higher coverages, whereas those for bond-breaking steps increase. This is consistent with simple ideas suggested from bond-order conservation where higher coverages lead to repulsive interactions between coadsorbed intermediates. This weakens the binding energies for both acetate

(19) Govind, N.; Peterson, M.; Fitzgerald, G.; King-Smith, D.; Andzelm, J. *Comput. Mater. Sci.* **2003**, *28*, 250.
(20) Hirshfeld, T. L. *Theor. Chim. Acta, B* **1977**, *44*, 129.
(21) Venkataraman, P. S.; Neurock, M.; Lusvardi, V. S.; Lerou, J. J.; Kragten, D. D.; van Santen, R. A. *J. Phys. Chem. B* **2002**, *106*, 1656.
(22) Venkataraman, P. S.; Neurock, M. *J. Catal.* **2000**, *191*, 301.
(23) Hansen, E. W.; Neurock, M. *J. Phys. Chem. B* **2001**, *105*, 9218.
(24) Desai, S. K.; Venkataraman, P.; Neurock, M. *J. Phys. Chem. B* **2001**, *105*, 9171.
(25) Stacchiola, D.; Azad, S.; Burkholder, L.; Tysoe, W. T. *J. Phys. Chem. B* **2001**, *105*, 11233.
(26) Kragten, D. D.; van Santen, R. A.; Neurock, M.; Lerou, J. *J. Phys. Chem. A* **1999**, *103*, 2756.
(27) Neurock, M. *J. Catal.* **2003**, *216*, 73.

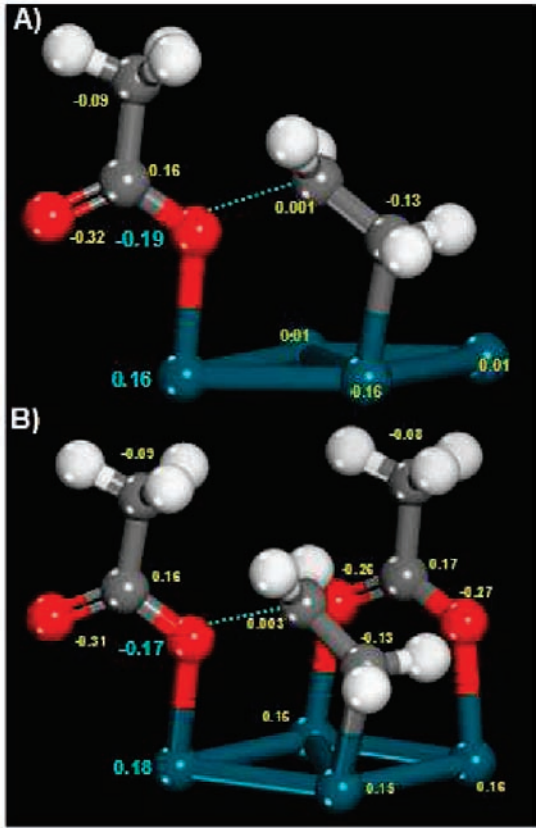

Figure 3. DFT-calculated Hirshfeld charges[20] on all of the atoms other than hydrogen for the isolated transition-state structures for the acetate−ethylene coupling reaction at: (a) low coverage (Θ = 1/9 ML of acetate) and (b) saturation acetate coverage (Θ = 1/3 ML of acetate).

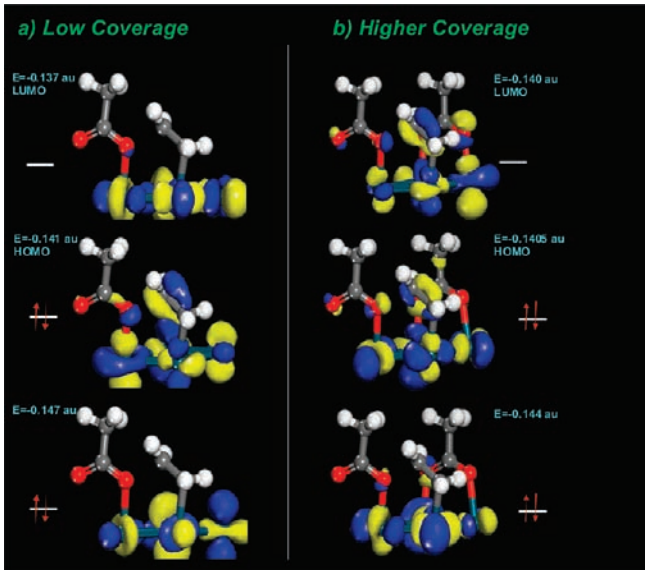

Figure 4. Frontier molecular orbitals of the transition state in the acetate−ethylene coupling reaction at: (a) low coverage (Θ = 1/9 ML of acetate) and (b) higher coverage (Θ = 1/3 ML of acetate). The antibonding σ^*_{C-O} state, which is occupied at low coverage, becomes unoccupied at higher coverages. All of the energies are reported in terms of atomic units (au).

and ethylene and thus favors the coupling and, more generally, bond-making processes.

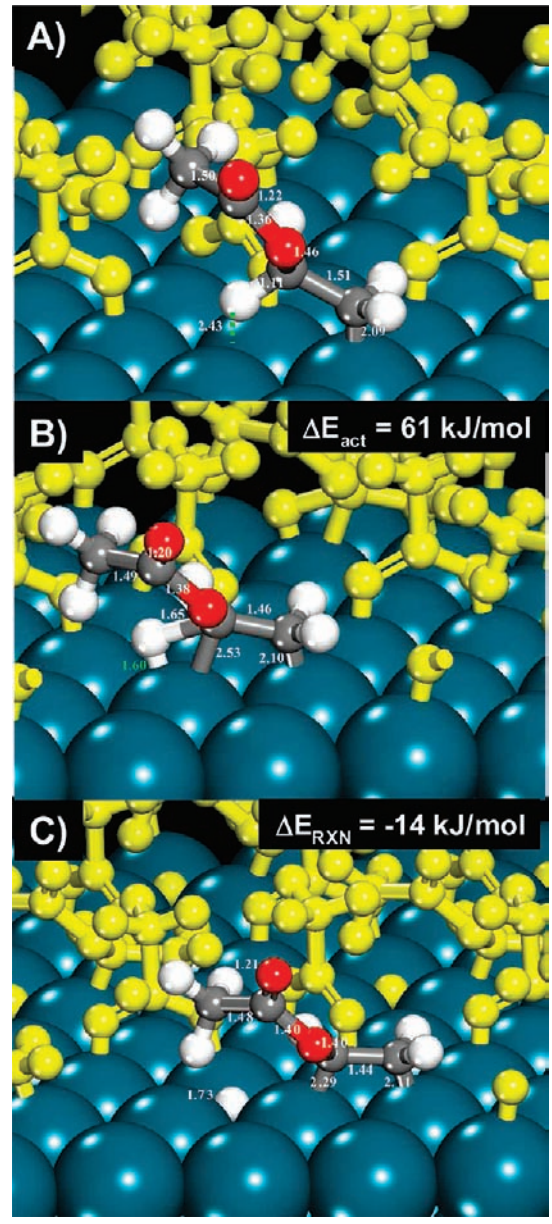

Figure 5. Optimized structures and energies for the coupling β-C−H activation of the acetoxyethyl intermediate at high (saturation) coverages (Θ = 1/3 ML of acetate). (A) Reactant, (B) transition, and (C) product states.

The activation barrier for the subsequent β-hydride elimination reaction was found to increase from +43 kJ/mol at low coverages (Θ = 1/9 ML) to +61 kJ/mol at a higher, saturation coverage (Θ = 1/3 ML). The structures and energies for reactant, transition, and product states at the full saturation coverage are shown in Figure 5. The transition state for the β-hydride elimination step involves a classic oxidative addition which proceeds via metal atom insertion into the C−H bond as depicted in Figure 5B. As might be expected, the transition state and the resulting activation barrier and overall reaction energy are quite similar to those found for the activation of the C−H bond of adsorbed ethyl.[18] This increase in the activation barrier is expected as the lateral interactions which result at higher coverages weaken the adsorbate bonding, which increases the barrier to dissociation. As the surface coverage of acetate is increased, there is a decrease in the electron-density on the carbon atom of the acetoxyethyl−palladium intermediate bound

Scheme 1. Illustrating the Samanos and Moiseev Pathways for the Formation of Vinyl Acetate Monomer Showing the Reaction Activation Energies (in kJ/mol) Calculated by DFT for Each Step

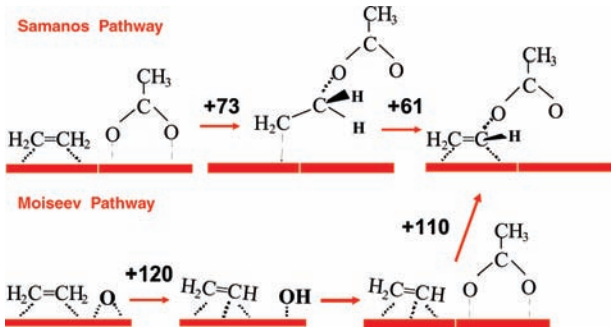

to the surface (similar to that which was found for the adsorbed acetate species). This decrease pushes the antibonding σ^*_{C-H} states higher in energy, thus making it more difficult to activate these bonds.

The vinyl acetate system discussed here nicely emphasizes the strong influence of coverage on the electronic structure of the transition states for the important coupling and dissociation steps and their effect on their activation barriers. Since the titration experiments to elucidate the reaction pathways on Pd(111) were carried out using saturated surfaces,[2] the high-coverage activation energies are used and summarized in Scheme 1. The results clearly show that, in all cases, the activation energies for the Samanos pathway are substantially lower than those for the Moiseev pathway and, as such, DFT predicts the correct reaction pathway.[2]

The activation energy calculated for the formation of the acetoxyethyl-palladium intermediate at 1/3 ML coverage (+73 kJ/mol) is somewhat higher than that for the subsequent β-hydride elimination step (61 kJ/mol), implying that, if the pre-exponential factors for the rate constant of both steps are similar, the rate constant for the first step should be lower than that for the second. However, the measurement of a large deuterium isotope effect indicates that the β-hydride elimination step is, in fact, rate limiting.[2] In addition, no acetoxyethyl intermediate is detected on the surface by infrared spectroscopy (at 1718 cm^{-1}) when the reaction is carried out using C_2H_4, but does appear when the β-hydride elimination step is slowed by using C_2D_4 instead of C_2H_4.[2] This implies that the coverage of the acetoxyethyl intermediate is sufficiently low when reacting C_2H_4 with adsorbed acetate species that the rate of the second step becomes rate limiting. The calculated heat of reaction to form the acetoxyethyl intermediate from acetate and ethylene is endothermic by 8 kJ/mol in accord with these observations. Thus, Scheme 1 predicts that the measured apparent activation energy should be the intrinsic activation barrier (61 kJ/mol) minus the heat or reaction for the coupling reaction (+8 kJ/mol) which is 53 kJ/mol.

The rate of reaction between adsorbed acetate and gas-phase ethylene was measured as a function of sample temperature and the results are displayed in Figure 6. Note that the reaction rate depends on ethylene pressure due to the pressure dependence of ethylene adsorption, and the data were collected with ethylene pressures that were sufficiently high (approximately 2×10^{-4} Torr) that no variation in reaction rate with ethylene pressure was observed. The data were fit using a simple kinetic model that assumes that ethylene adsorption is blocked by surface acetate species as expected from their structures,[3,4] and that the reaction rate is given by $k \times \Theta(\text{ethylene}) \times \Theta(\text{acetate})$, where

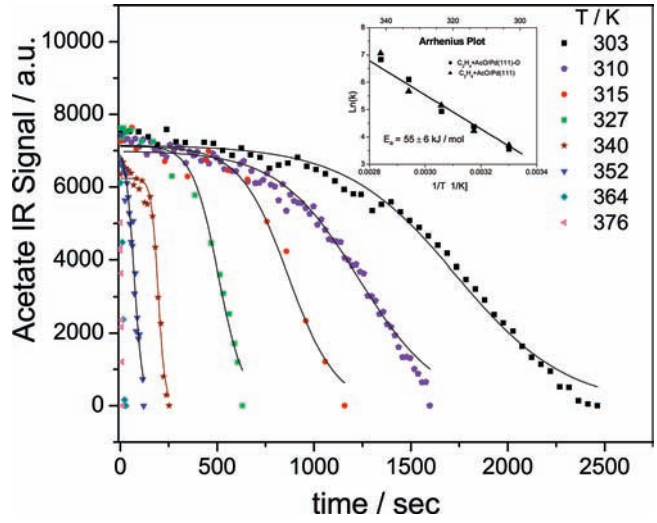

Figure 6. Plot of the acetate coverage as a function of temperature for the removal of acetate species by gas-phase ethylene at various temperatures. Shown as an inset is an Arrhenius plot of ln(k) versus 1/T.

Θ refers to the surface coverage, which allows the titration curves to be fit to an analytical function that enables the reaction rate constant to be obtained as a function of temperature.[2] This fit to the data with a single rate constant (shown as solid line of the experimental data), and the agreement is good up to an acetate coverage of ~30% of saturation and appears to deviate somewhat at lower coverages. The reaction rate constant might be expected to change as the acetate species are removed due to the effects of coverage on the activation energies referred to above. However, the surface is completely saturated throughout the course of the reaction since the ethylene and acetic acid react to form VAM, and ultimately any vacant surface sites that arise are readily removed as a result of ethylidyne formation.[2] Thus, while the environment around the reaction center is changing during the titration experiment, the coverage remains constant. The lateral interactions thus result in reasonably constant reaction kinetics. The complex effects of the reaction environment are currently being explored using Monte Carlo kinetics simulations.

The resulting Arrhenius plots of ln(k) versus 1/T, where T is the sample temperature are shown as an inset to Figure 6 for oxygen-covered (⟨564⟩) and clean Pd(111) (⟨97⟩). The Arrhenius plots are essentially identical, revealing that oxygen does not substantially affect the reaction kinetics and yields a reaction activation energy of 55 ± 4 kJ/mol, in very good agreement with the calculated value of 53 kJ/mol. This indicates that DFT can calculate fairly reliable reaction activation energies for even relatively complex surface reactions and also emphasizes the effect of environment on the activation energy, showing significant variations as a function of coverage. Such changes in activation energy with coverage have a very important effect on the way in which reaction kinetics must be modeled.

Conclusions

Density functional theory analyses of the activation energies for the elementary steps in the Samanos pathway for the synthesis of vinyl acetate monomer show that the activation energies critically depend on surface coverage. The ability to accurately predict experimental barriers thus requires the determination of surface coverages that form under experimental

conditions. The electronic origins of these coverage effects are explored by examining the evolution of frontier molecular orbitals from the reactant to the transition state. The activation energy for the rate-limiting β-hydride elimination reaction from the acetoxyethyl intermediate calculated at saturation coverage is compared with experimental measurements of the rate of titration of a saturated acetate overlayer as a function of temperature where the acetate coverage is measured using infrared spectroscopy. It is found that the acetate coverage as a function of time can be modeled using a single rate constant up to an acetate coverage that is ~30% of saturation. The experimentally measured activation energy (55 ± 4 kJ/mol) is in good agreement with the calculated apparent activation energy of 53 kJ/mol. A detailed analysis of the changes in the atomic charges and the occupation of the frontier orbitals indicate that higher acetate coverages lower the electron density on the oxygen, making it less nucleophilic, and decrease the occupation of the antibonding C−O σ^* state which lowers the activation energy.

Acknowledgment. We gratefully acknowledge support of this work by the U.S. Department of Energy, Division of Chemical Sciences, Office of Basic Energy Sciences, under Grant No. DE-FG02-92ER14289. We also kindly acknowledge the computational resources provided by the EMSL, a national scientific user facility sponsored by the Department of Energy's Office of Biological and Environmental Research and located at Pacific Northwest National Laboratory

JA907061M